Available online at www.sciencedirect.com
SCIENCE DIRECT®
Advances in Space Research 34 (2004) 578–582
ADVANCES IN SPACE RESEARCH (a COSPAR publication)
www.elsevier.com/locate/asr

# Simulations of cosmological observations with ASTRO-F/FIS

Woong-Seob Jeong [a], Soojong Pak [a,b,*], Hyung Mok Lee [a], Takao Nakagawa [c], Masaru Watanabe [c], Mitsunobu Kawada [d], Hiroshi Shibai [d], Chris Pearson [e], Michael Rowan-Robinson [e]

[a] Graduate School of Earth and Environmental Sciences, Seoul National University, Shillim-Dong, Kwanak-Gu, Seoul 151-742, Republic of Korea
[b] Korea Astronomy Observatory, Whaam-Dong, Youseong-Gu, Taejeon 305-348, Republic of Korea
[c] Institute of Space and Astronautical Science, Yoshinodai 3-1-1, Sagamihara, Kanagawa 229-8510, Japan
[d] Graduate School of Science, Nagoya University, Furo-cho, Chigusa-ku, Nagoya 464-8602, Japan
[e] Astrophysics Group, Imperial College of Science Technology and Medicine, London SW7 2BZ, UK

Received 18 February 2003; received in revised form 25 March 2003; accepted 4 April 2003

**Abstract**

The far-infrared surveyor (FIS) is one of the focal-plane instruments on the ASTRO-F mission which will be launched in early 2004. The purpose of the FIS is to perform an all-sky survey in the wavelength range 50–200 μm. We are developing a suite of software that simulates the observations with this instrument to check the performance of the ASTRO-F/FIS as a whole and to prepare input data sets for the data analysis and reduction software prior to launch. The detection limit of the FIS is affected by many factors: the performance of the entire system, the brightness of sky and telescope emission, readout process, and the distribution of the celestial sources. The input model for FIS simulator consists of a catalogue of extragalactic point sources generated from the luminosity function at 60 μm, and a redshift distribution incorporating pure luminosity evolution ($\Omega_0 = 1,\ \Lambda = 0$). We present the expected source count results from the FIS survey and estimate the limiting redshift as ~2.5 in the band at 50–110 μm and ~3 in the band at 110–200 μm.


*Keywords:* ASTRO-F; Far-infrared surveyor; Image processing techniques; Photometry of galaxies; Cosmological observations; Infrared observations of galaxies

## 1. Introduction

The ASTRO-F (previously known as IRIS) is the second Japanese space mission for infrared astronomy which will be launched in early 2004 (Murakami, 1998; Shibai, 2001; Nakagawa, 2001). The major task of this mission is to carry out an all sky survey using the far-infrared surveyor (FIS), in four far-infrared bands, i.e., N60 (50–75 μm), WIDE-S (50–110 μm), N170 (150–200 μm), and WIDE-L (110–200 μm). The detailed hardware specifications of the FIS are described in Kawada (1998, 2000).

The performance of ASTRO-F/FIS can be represented by the effective detection limit for faint sources which are mostly distant galaxies and seen as point-like sources. There are several factors contributing to the effective detection limits. The sensitivity of the detectors (e.g., read noise) and the entire telescope system (e.g., photon noise of the telescope emission) allows only sources brighter than a certain threshold to be reliably measured. In addition, the structure of the cirrus emission from the Galaxy contributes to the photon noise and the sky confusion noise. Moreover, the measurement of the brightness of a source can be further influenced by neighboring sources if more than one source lies within a single beam of the telescope. The final detection limit should thus depend on the performance of the entire system, the brightness of sky and telescope emission, readout process, and the distribution of sources as a function of the flux.

We have constructed a software simulator called the FISVI representing Virtual Instrument of the FIS, that can simulate the data stream of ASTRO-F/FIS. The

* Corresponding author. Tel.: +82-42-865-3248; fax: +82-42-861-5610.
*E-mail address:* soojong@kao.re.kr (S. Pak).

0273-1177/$30 © 2004 COSPAR. Published by Elsevier Ltd. All rights reserved.
doi:10.1016/j.asr.2003.04.040

purposes of the software simulation are to confirm the hardware configurations and to measure the detection limits. The initial design concepts and the detailed algorithms of the FISVI are described in Jeong et al. (2000, 2003). Anomalous behaviours of the detectors are discussed in Jeong et al. (2004). In this paper, we assumed that the sky brightness is constant and only contributes photon noise. The sky confusion noise due to the cirrus structure will be discussed in the following paper.

## 2. Software structure

Fig. 1 shows an overview of the simulation software. We first prepare input data for the observing simulations. The input data file provides the coordinates and the properties of the sources, e.g., type of spectral energy distribution (SED), luminosity and redshift, in the virtual sky. We only deal with point sources in this paper because most of the target sources will be distant. The observing simulation procedure makes the images on the focal plane by convolving the point sources and the point spread function (PSF) of the telescope and the instrument. In this convolution, we use the compiled PSF which includes the information on the transmittance and the spectral response in order to reduce the computation time by an order of magnitude (Jeong et al., 2003). The software generates time series data for each pixel by simulating the scanning procedure of the ASTRO-F/FIS survey mode observations. Using these time series data, we can simulate an image through the image reconstruction routines. We finally count the sources on the reconstructed images to estimate the detection limits.

## 3. Point source catalogue

In our previous work (Jeong et al., 2003), we did not consider in detail, the SEDs of galaxy sources, their evolution, or the cosmological model for the spatial distribution of the input sources. However, these results showed that the effective detection limits in the long wavelength bands, e.g., WIDE-L band, are governed by source confusion noise. In order to check the detection limits of the ASTRO-F/FIS with realistic extragalactic, cosmological models, we introduce a point source catalogue generated from the models of Pearson and Rowan-Robinson (1996), Pearson (2001) and Rowan-Robinson (2001).

### 3.1. Galaxy evolution models

Generally, the source count model can be described by the SEDs of galaxies and their luminosity function (see Fig. 2), if there is no evolution of the galaxies. In this simulation, we incorporate four spectral components: infrared cirrus to represent quiescent normal galaxies, an M82-like starburst, an Arp 220-like high optical depth starburst to represent ultraluminous infrared galaxies, and an active galactic nucleus (AGN) dust torus (Rowan-Robinson, 2001). The 60 μm luminosity function is determined by using the IRAS PSCz sample (Saunders et al., 2000).

It has been known that galaxy evolution is a necessary and crucial ingredient in explaining the source counts at infrared wavelengths. Evolution can be in the luminosity or/and in the number density of the source population. The effect of luminosity evolution, assumed to be due to enhanced bulk star formation in galaxies, is to make the luminosity of the galaxies increase with look back time, i.e., galaxies were more luminous in the past. The effect of the density evolution, assumed to be due to merging in the galaxy population, is to increase the number density of galaxies with look back time, i.e., galaxies were more numerous in the past. The luminosity evolution can be represented parametrically as power law functions. We assume the luminosity of a source increases by a factor $f(z)$ at a redshift z, i.e., $L(z) = L(z = 0)f(z)$, where $f(z)$ follows the power law function of redshift $z$ (Pearson and Rowan-Robinson,

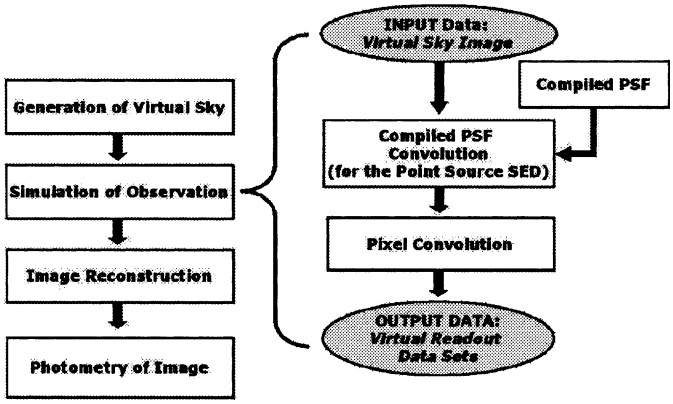


Fig. 1. Structure of the simulation software. On the right side, the virtual observation procedures using the compiled PSF are shown.

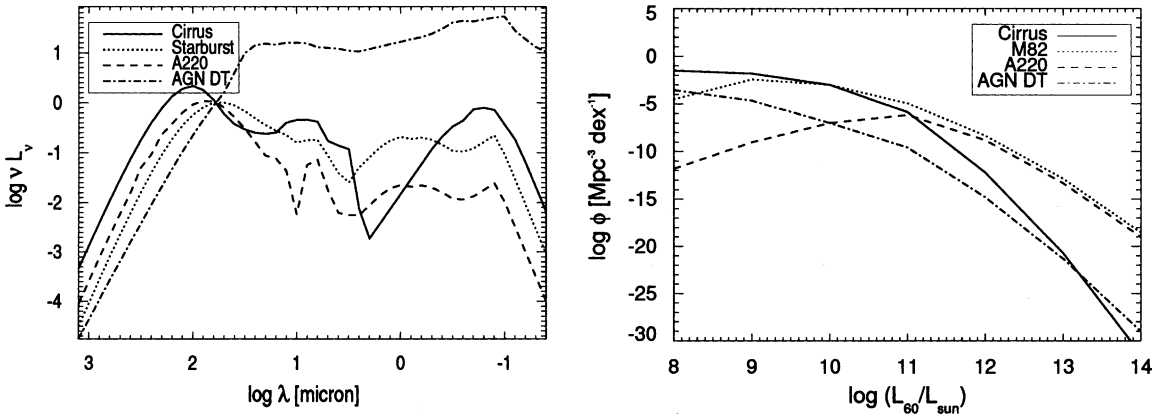


Fig. 2. Spectral energy distribution (left: Rowan-Robinson, 2001) and luminosity function (right: Saunders et al., 2000) at 60 μm for four galaxy types used in this simulation.

1996): $f(z) = (1+z)^{3.1}$ for $0 < z \leqslant 2$, $f(z=2)^{3.1}$ for $2 < z < 10$, and 0 for $z \geqslant 10$. Similarly, the density evolution also follows the power law (Rowan-Robinson, 2001): $\rho(z) = \rho(0)(l+z)^n$, where $n = 1$.

## 4. Source distribution

For any source at redshift $z$, the rest frame source luminosity, $L_{\nu_o}$, at frequency, $\nu_o$, is spread out over a sphere of surface $4\pi D_L^2$ where $D_L$ is the luminosity distance which is a distance to a source as determined by observing the attenuation of the source's light intensity. The observed flux at the observing frequency $\nu$ is obtained from

$$S(\nu) = \frac{(1+z)L_{\nu_o}}{4\pi D_L^2} = \frac{L_\nu K(L,z)}{4\pi D_L^2}, \tag{1}$$

where $K(L,z)$ is the $K$-correction that relates the rest frame source spectrum to the observers frame source spectrum. For any given flux limit, we then calculate the limiting luminosity, $L$ for a source to be observable at a redshift $z(L,S,\nu)$. The total number of sources down to a flux limit $S$ is then calculated by summing over the 60 μm luminosity function and cosmological volume element as given by

$$N_\nu(>S) = \sum_{i=1}^{4} \int d\log L \int_o^{z(L,S,\nu)} \phi(L,z)\,\mathrm{d}V, \tag{2}$$

where $\phi$ is the luminosity function and the summation is performed for four types of SED.

## 5. Galaxy source counts results

We make the input point source catalogue from the source distribution and generate the image for each band. We carried out the aperture photometry on the simulated images using SExtractor software $v2.0.0$ (Bertin and Arnouts, 1996). The source detection in this simulation mainly depends on the photon and readout noise, and the source confusion noise.

In this work, we assumed three sources of noise: photon noise due to the sky background, photon noise due to the thermal emission from the telescope, and readout noise. We assumed that the photon noise and the readout noise follow Poisson statistics and Gaussian statistics, respectively (see Jeong et al., 2003 for details). In addition, the detection limit is affected by the source confusion: many detected sources contain fainter sources within the beam. In order to compare this with the theoretical source confusion limit, we also calculate the theoretical $5\sigma$ source confusion noise using the formula in Condon (1974) and Franceschini et al. (1989), and plots that in Figs. 3 and 4.

Fig. 3 shows a plot of the $S_{out}/S_{in}$ as a function of $S_{in}$, where $S_{in}$ and $S_{out}$ denote the input flux and the flux obtained by photometry. We find that the output flux $S_{out}$ is consistent with the input flux for the SW bands. The theoretical source confusion limit is much lower than the level of the photon and readout noise. But, in the LW bands, the output flux $S_{out}$ is systematically overestimated for sources below the theoretical source confusion limits. Such an upward bias is caused by source confusion. These results mean that the source confusion in the SW bands is negligible, but in the LW bands it will affect source detection.

Fig. 4 shows a plot of integrated source count results. The source distribution in the LW bands has a higher normalization factor due to the strong evolution and the SED of galaxies compared with our previous work (Jeong et al., 2003), which make the source confusion limits higher. The bend at low $S$ is mainly due to the detection limit dominated by the photon and readout noise in the SW bands. Because the theoretical source confusion limit is larger than the bend in LW bands, source confusion becomes important in the LW bands

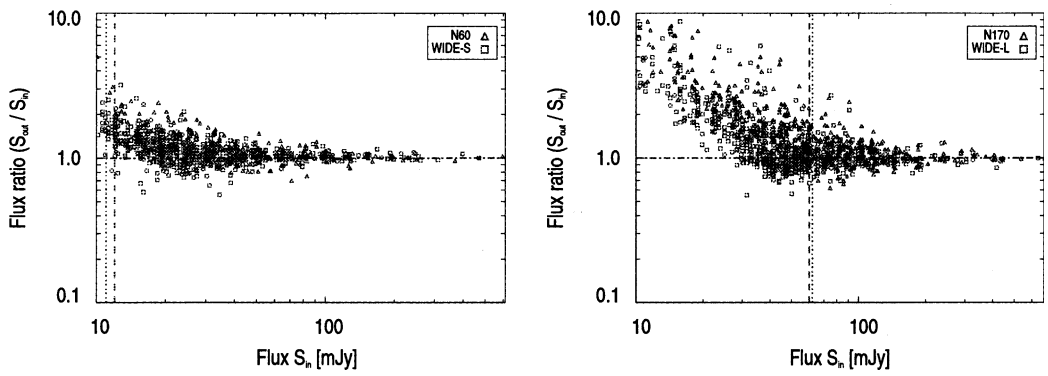


Fig. 3. Flux ratio between the input and the output fluxes for extracted and identified sources. The vertical lines represent the theoretical $5\sigma$ source confusion noise using the formula for the narrow band (dotted line) and the wide band (dashed line). The output flux is well consistent with the input flux in the case of SW bands (left). But, in LW bands, the output flux is greater than the input flux (right) due to the source confusion.

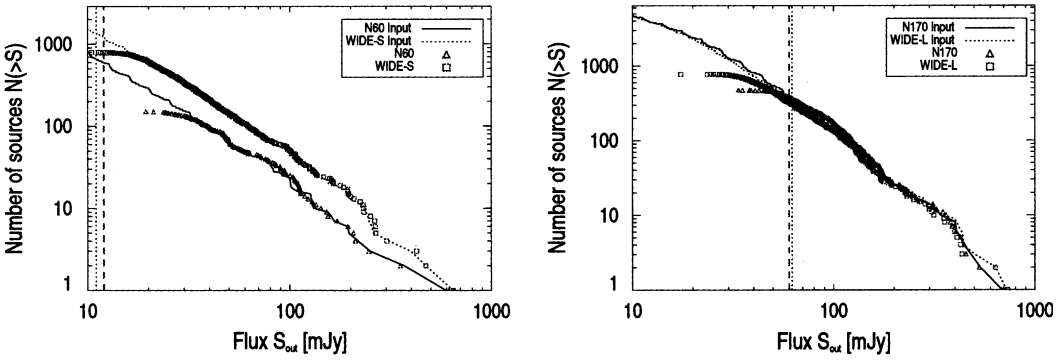


Fig. 4. Integrated source count results. The left panel is for SW bands and the right panel is for LW bands. The vertical lines mean the theoretical confusion limits.

Table 1
$5\sigma$ detection limits

| | WIDE-L (mJy) | N170 (mJy) | WIDE-S (mJy) | N60 (mJy) |
|---|---|---|---|---|
| Source confusion limit (Jeong et al., 2003) | 23 | 24 | 12 | 11 |
| Source confusion limit (present) | 60 | 62 | 13 | 12 |
| Detection limit (Jeong et al., 2003) | 26 | 66 | 21 | 49 |
| Detection limit (present) | 54 | 78 | 23 | 46 |

though we can not see a significant flux boosting in the right panel of Fig. 4. Therefore, the source count result is limited in SW bands by the photon and readout noise and in LW by the source confusion. Table 1 shows the $5\sigma$ detection in our simulation. For comparison, we also list the previous work (Jeong et al., 2003).

## 6. Discussion

In order to check the performance of the FIS survey, we have estimated the predicted number-redshift distribution in a cosmological model. We define the detection correctness which is the ratio of the number of correctly detected sources to the number of actually detected sources to calculate the detection limits. This sets a lower limit to the luminosity of an observable source at redshift $z$. The number-redshift distribution at flux $S$, can be obtained from the integration of the evolving luminosity function and is given by

$$\frac{\mathrm{d}N_\nu(S,z)}{\mathrm{d}z} = \int d\log L \int_{\mathrm{o}}^{z(L,S,\nu)} \phi(L,z)\frac{\mathrm{d}V}{\mathrm{d}z}. \quad (3)$$

Source detection is mainly limited by photon and readout noise in the SW bands. Since the source confusion severely affects source detection in the LW bands due to the crowded beams, its limiting magnitude is not so different from that of the SW bands (see Fig. 5). The limiting redshift is $\sim$2.5 in SW bands and $\sim$3 in LW bands. Also, we can see that the number of sources with high redshift in the LW bands is larger than that in the SW bands. This is due to the positive effects of the large $K$-corrections induced as the LW bands climb the Rayleigh–Jeans slope towards the dust peak around 100–60 μm in the source SEDs.

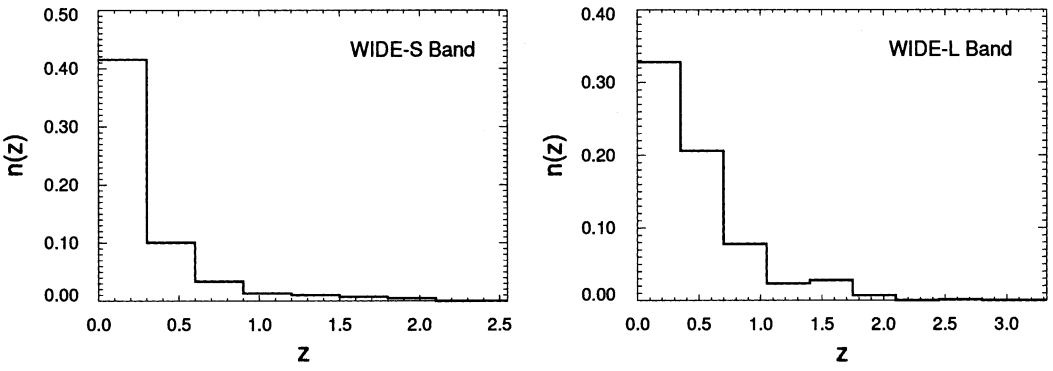


Fig. 5. Predicted redshift distribution.

## Acknowledgements

W.-S. Jeong was financially supported by the BK21 Project of the Korean Government. This work was financially supported in part by the KOSEF-JSPS corporative program. The ASTRO-F project is managed and operated by the Institute of Space and Astronautical Science (ISAS), Japan in collaboration with groups in universities and institutes in Japan as well as with Seoul National University, Korea.

## References

Bertin, E., Arnouts, S. Extractor: software for source extraction. Astron. Astrophys. Suppl. Ser. 117, 393–404, 1996.

Condon, J.J. Confusion and flux–density error distribution. Astrophy. J. 188, 279–286, 1974.

Franceschini, A., Toffolatti, L., Danese, L. Discrete source distributions to small-scale anisotropies of the microwave background. Astrophys. J. 344, 35–45, 1989.

Jeong, W.-S., Pak, S., Lee, H.M., et al., Observing simulations of far-infrared surveyor: design overview and current status, in: Matsumoto, T., Shibai, H. (Eds.), Mid- and Far-Infrared Astronomy and Future Missions. ISAS Report SP14, pp. 297–304, ISAS, Sagamihara, Japan, 2000.

Jeong, W.-S., Pak, S., Lee, H.M., Nakagawa, T., Sohn, J., Ahn, I., Yamamura, I., Watanabe, M., Kawada, M., Shibai, H. ASTRO-F/FIS observing simulation: detection limits for point sources. P. Astron. Soc. Jpn. 55, 717–731, 2003.

Jeong, W.-S., Pak, S., Lee, H.M., et al. ASTRO-F/FIS observing simulation including detector characteristics. Adv. Space Res., 2004 (this issue) doi: 10.1016/j.asr.2003.04.043.

Kawada, M., FIS: Far-infrared surveyor onboard IRIS, in: Fowler, A.M. (Ed.), Infrared Astronomical Instrumentation. Proc. of SPIE, Washington, USA, vol. 3354, pp. 905–914, 1998.

Kawada, M., FIS – far-infrared surveyor onboard the ASTRO-F. in: Matsumoto, T., Shibai, H. (Eds.), Mid- and Far-infrared Astronomy and Future Missions. ISAS Report SP14, pp. 273–280, ISAS, Sagamihara, Japan, 2000.

Murakami, H., Japanese infrared survey mission IRIS (ASTRO-F), in: Belly, P.Y., Beckingridge, J.B. (Eds.), Space Telescopes and Instruments V, Proc. of SPIE, Washington, USA, vol. 3356, pp. 471–477, 1998.

Nakagawa, T. ASTRO-F survey as input catalogues for FIRST, in: Pilbratt, G.L., Cernicharo, J., Heras, A.M., Prusti, T., Harris, R. (Eds.), The Promise of the Herschel Space Observatory. ESA-SP 460, pp. 67–74, ESA Publications Division, Noordwijk, Holland, 2001.

Pearson, C.P., Rowan-Robinson, M. Starburst galaxy contributions to extragalactic source counts. Mon. Not. R. Astron. Soc. 283, 174–192, 1996.

Pearson, C.P. Evolutionary constraints from infrared source counts. Mon. Not. R. Astron. Soc. 325, 1511–1526, 2001.

Rowan-Robinson, M. The star formation history of universe: an infrared perspective. Astrophys. J. 549, 745–758, 2001.

Saunders, W., Sutherland, W.J., Maddox, S.J., et al. The PSCz catalogue. Mon. Not. R. Astron. Soc. 317, 55–63, 2000.

Shibai, H. The ASTRO-F (IRIS) mission, in: Harwit, M., Hauser, M.G. (Eds.), The Extragalactic Background and its Cosmological Implications. IAU Symposium No. 204, pp. 455–466, Astronomical Society of the Pacific, Michigan, USA, 2001.